

# High Nuclearity Ruthenium Carbonyl Cluster Chemistry. 5.<sup>1</sup> Local Density Functional, Electronic Spectroscopy, Magnetic Susceptibility, and Electron Paramagnetic Resonance Studies on (Carbido)decaruthenium Carbonyl Clusters

Marie P. Cifuentes,<sup>†</sup> Mark G. Humphrey,<sup>\*,‡</sup> John E. McGrady,<sup>‡</sup> Paul J. Smith,<sup>‡</sup> Robert Stranger,<sup>‡</sup> Keith S. Murray,<sup>§</sup> and Boujemaa Moubaraki<sup>§</sup>

Contribution from the Department of Chemistry, University of New England, Armidale, NSW 2351, Australia, Department of Chemistry, Australian National University, Canberra, ACT 0200, Australia, and Department of Chemistry, Monash University, Clayton, Vic 3168, Australia

Received January 22, 1996<sup>⊗</sup>

**Abstract:** Electronic spectra of “giant tetrahedral” decaruthenium cluster anions are consistent with a HOMO–LUMO gap of  $\leq 1.2$  eV, with intense transitions assigned to  $M-M^* \rightarrow CO\ 2\pi^*$  at high energy and weak transitions assigned to  $M-CO\ \pi \rightarrow M-CO\ \sigma^*$  at low energy; the former are relatively insensitive to increasing phosphine substitution or cluster core charge, whereas the latter show some ligand dependence. The first diffuse reflectance UV-vis-NIR spectra of metal carbonyl clusters have been obtained; spectra of  $[Ru_2(\mu-H)(\mu-NC_5H_4)_2(CO)_4(NC_5H_5)_2]$ – $[Ru_{10}(\mu-H)(\mu_6-C)(CO)_{23}(PPh_3)]$  and  $[ppn]_2[Ru_{10}(\mu_6-C)(CO)_{24}]$  contain broad absorptions extending to a  $\lambda_{onset}$  of 1300 nm with absorption maxima corresponding to those of the solution spectra superimposed. Local density functional (LDF) calculations support the optical spectra assignments and predict a triply degenerate HOMO approximately 1.3 eV below the LUMO. Magnetic susceptibility data for  $[Ru_2(\mu-H)(\mu-NC_5H_4)_2(CO)_4(NC_5H_5)_2][Ru_{10}(\mu-H)(\mu_6-C)(CO)_{23}(PPh_3)]$  show a temperature independent susceptibility  $\chi_m$  of  $+1384 \pm 10 \times 10^{-6}$  cm<sup>3</sup> mol<sup>-1</sup> (diamagnetic correction including decaruthenium valence electrons), arising from Van Vleck paramagnetism; unlike related decaosmium clusters and lower nuclearity ruthenium clusters, no temperature dependent component of the susceptibility exists. Electron paramagnetic resonance (EPR) investigations on three decaruthenium cluster anions reveal a temperature-independent paramagnetic (TIP) signal which does not derive from solid-state packing effects, the nature of the cation, the presence of impurities such as colloids, particles, or oxides, or incipient metallic character (“mesometallic” behavior); this EPR signal, the first reported TIP resonance from a carbonyl cluster, is assigned to the presence of radical decaruthenium clusters due to oxidation of the cluster anions. Unlike high-nuclearity clusters examined previously by EPR, no temperature-dependent response was found for  $[Ru_2(\mu-H)(\mu-NC_5H_4)_2(CO)_4(NC_5H_5)_2][Ru_{10}(\mu-H)(\mu_6-C)(CO)_{24}]$ . The electronic spectroscopy, magnetic susceptibility data, EPR studies, and LDF calculations are consistent with these high-nuclearity carbonyl clusters having “molecular” rather than “mesometallic” character.

## Introduction

The physical properties of metal cluster compounds have been the subject of active investigation recently, largely due to interest in the transition from molecular to bulk metallic behavior which should ensue upon increasing cluster size.<sup>2</sup> Early assumptions regarding a smooth transition from molecular to bulk properties were subsequently modified to incorporate the existence of an intermediate “metametallic”<sup>3</sup> or “mesometallic”<sup>4</sup> regime, possessing properties distinct from those of the molecular and bulk domains. The mesometallic region of cluster core nuclearities

is dependent upon metal, temperature, and the physical property one is studying. The location of the mesometallic domain is thus relatively diffuse and ill-defined; recent results suggest that molecules with medium- to high-nuclearity cluster cores may have mesometallic character and that some bulklike metallic properties may be acquired by larger ligated high-nuclearity metal clusters with “inner core” metal atoms, the electron-depleting influence of ligation being essentially restricted to the “surface” metal atoms.<sup>5</sup>

In the quest to define the onset of metallic character, a range of physical properties have been assayed. Interest in the evolution of metallic properties with cluster size has led some investigators to examine electronic absorption spectra (UV-vis-NIR), as a potential source of information on electronic structure and bonding.<sup>6</sup> Large molecular metal clusters are usually very dark and show rich UV-visible spectra; although pronounced peaks are evident in these spectra, the absorption bands are also very broad, due to the large number of statically and vibronically

\* To whom correspondence should be addressed. Department of Chemistry, Australian National University, Canberra, ACT 0200, Australia. Ph: +61 6 249 2927. Fax: +61 6 249 0760. E-mail: Mark.Humphrey@anu.edu.au.

<sup>†</sup> University of New England.

<sup>‡</sup> Australian National University.

<sup>§</sup> Monash University.

<sup>⊗</sup> Abstract published in *Advance ACS Abstracts*, December 15, 1996.

(1) Part 4: Cifuentes, M. P.; Humphrey, M. G.; Willis, A. C. J. *Organomet. Chem.* **1996**, *513*, 85–95.

(2) (a) *Clusters and Colloids: From Theory to Applications*; Schmid, G., Ed.; VCH: Weinheim, 1994. (b) *Physics and Chemistry of Metal Cluster Compounds*; de Jongh, L. J., Ed.; Kluwer: Dordrecht, 1994.

(3) Benfield, R. E. J. *Phys. Chem.* **1987**, *91*, 2712–6.

(4) de Jongh, L. J. In *Physics and Chemistry of Metal Cluster Compounds*; de Jongh, L. J., Ed.; Kluwer Academic Publishers: Dordrecht, 1994; pp 1–39.

(5) (a) Mulder, F. M.; Stegink, T. A.; Thiel, R. C.; de Jongh, L. J.; Schmid, G. *Nature* **1994**, *367*, 716–8. (b) van Leeuwen, D. A.; van Ruitenbeek, J. M.; de Jongh, L. J.; Ceriotto, A.; Pacchioni, G.; Häberlein, O. D.; Rösch, N. *Phys. Rev. Lett.* **1994**, *73*, 1432–5.

(6) Benfield, R. E. In *Physics and Chemistry of Metal Cluster Compounds*; de Jongh, L. J., Ed.; Kluwer Academic Publishers: Dordrecht, 1994; pp 264–70.

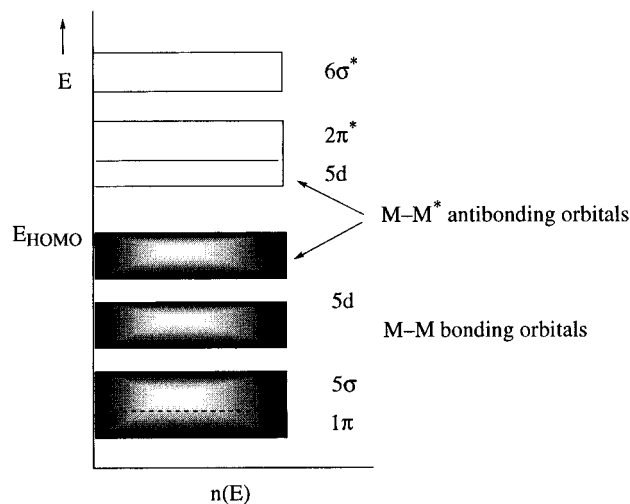


**Figure 1.** Energy level diagram of small transition-metal carbonyl clusters (Adapted with permission from ref 10). Copyright 1987 American Chemical Society.

allowed transitions occurring when light interacts with a cluster of even moderate size. Theoretical attempts to interpret the spectra are rendered extremely complex, although some success has been reported using a local density approximation on some osmium carbonyl<sup>7</sup> and nickel<sup>8</sup> clusters. The broad continuous electronic absorption band that evolves as cluster nuclearity increases reflects the overall density of states of the electronic energy levels in the cluster; the small molecule HOMO then approaches the Fermi energy of bulk metal. At the low-energy end of the spectrum, the onset wavelength,  $\lambda_{\text{onset}}$ , has been used to estimate the “band gap” energy difference between the HOMO and LUMO in the cluster.<sup>6</sup>

Electronic absorption spectra of small clusters such as  $[\text{Os}_3(\text{CO})_{12}]$  have been assigned by X $\alpha$  MO treatments.<sup>6</sup> The energy level diagram of a schematic density of states for the medium-nuclearity cluster  $[\text{Os}_6(\text{CO})_{18}]$  has been constructed from solution visible absorption spectra and gas-phase photoemission studies, together with chemical pseudopotential calculations (Figure 1); it is believed to be a reasonable representation of the density of states of metal cluster carbonyls in general<sup>9</sup> and has been used to interpret the spectrum of  $[\text{Os}_{10}(\mu_6\text{-C})(\text{CO})_{24}]^{2-}$ .<sup>10</sup> Substantial absorptions in the spectrum of the high-nuclearity cluster  $[\text{Os}_{10}(\mu_6\text{-C})(\text{CO})_{24}]^{2-}$  at about 230 nm ( $\Delta E_{\text{max}} \approx 5.4$  eV) have been assigned to transitions from M-M bonding orbitals in the lower half of the d band into the carbonyl  $\pi^*$  orbitals and do not appear to be cluster nuclearity dependent from studies in the osmium system.<sup>10</sup> In contrast, peaks at 420–540 nm ( $\Delta E \approx 2.3$ –2.9 eV) were assigned to transitions from the upper part of the d band (the M-M\* levels) into the carbonyl  $2\pi^*$  levels and split into two features on fusing  $\text{Os}_{10}$  cores into the  $[\text{Os}_{18}\text{Hg}_3(\mu_6\text{-C})_2(\text{CO})_{48}]^{2-}$  “linked” cluster. In all the osmium clusters studied ( $[\text{Os}_6(\text{CO})_{18}]$ ,  $[\text{Os}_{10}(\mu_6\text{-C})(\text{CO})_{24}]^{2-}$ ,  $[\text{Os}_{11}\text{C}(\text{CO})_{27}]^{2-}$ ,  $[\text{Os}_{10}(\mu_6\text{-C})(\text{CO})_{24}\text{I}_2]$ , and  $[\text{Os}_{18}\text{Hg}_3(\mu_6\text{-C})_2(\text{CO})_{48}]^{2-}$ ), optical absorption becomes negligible for wavelengths greater than 830 nm ( $\Delta E \approx 1.5$  eV), from which it has

been suggested that the HOMO–LUMO gap is about 1 eV, raising the possibility that the electronic ground state structures may be high spin and paramagnetic.<sup>6</sup> For these large clusters, resolution of electronic bands is lost, and a broad, continuous electronic absorption evolves, spanning the visible region into the near-infrared and resembling “interband” transitions of the corresponding metal.

A further physical property that has attracted considerable attention is magnetism, and results thus far are the subject of some controversy. Small even-electron molecules are diamagnetic, while bulk metals exhibit temperature-independent (Pauli) paramagnetism. In the mesometallic realm, a temperature-dependent (Curie) paramagnetism resulting from quantum-size effects has been predicted when the HOMO–LUMO gap is of the order of  $kT$ .<sup>11</sup> The magnetic properties of metal cluster complexes have been probed by both magnetic susceptibility measurements and electron paramagnetic resonance (EPR) spectroscopy. Magnetic susceptibility measurements on microcrystalline samples of medium- to high-nuclearity clusters of osmium,<sup>12</sup> platinum,<sup>13</sup> and nickel<sup>13a</sup> reveal Curie paramagnetism at low temperatures, consistent with mesometallic character, together with temperature-independent (Van Vleck) paramagnetic contributions which increase monotonically with cluster core size. More recent results by van Leeuwen *et al.*<sup>5b</sup> on both nickel clusters and nickel-platinum mixed-metal clusters as single crystals ascribe the measured Curie-type responses to a variety of possibilities (particle surface contamination, deviations from exact stoichiometry, variable number of interstitial hydrides, positional isomerism of Pt and Ni); the carbonyl ligation is suggested to completely quench the magnetic moments of the surface metal atoms in these clusters. These results emphasize the experimental difficulties in this area; as previous reports dealt with a wide range of metals, ligands, cluster nuclearities and geometries, and involved materials of very high purity, it is not certain that all Curie responses arise from such contaminants, and considerable controversy remains.

As mentioned above, magnetism has also been assessed by EPR spectroscopy; results with even-electron osmium<sup>3,12,14</sup> and rhodium<sup>15</sup> clusters have been reported. Osmium clusters with less than ten metal atoms show no EPR signals, while those of higher nuclearity have an EPR signal exhibiting temperature-dependent Curie or Curie–Weiss behavior.<sup>14</sup> Similarly, studies with  $[\text{Rh}_17\text{S}_2(\text{CO})_{32}]^{3-}$  found a low temperature Curie response. Thus, the temperature dependence of EPR signals from even-electron high-nuclearity clusters has exhibited Curie behavior only, consistent with a mesometallic regime arising from quantum-size effects; no reports of temperature-independent signals have appeared.

Previous work has shown that the onset of mesometallic properties is metal-dependent; some metals should approach metallic behavior at lower nuclearity than others. Magnetic susceptibility studies of small ( $M_n$ ,  $n = 3$ –6) ruthenium clusters have been reported<sup>16</sup> and show that clusters containing four to six metal atoms exhibit low temperature Curie-type susceptibility, together with a temperature-independent contribution. In

(11) Edwards, P. P.; Sienko, M. J. *Int. Rev. Phys. Chem.* **1983**, *3*, 83–137.

(12) (a) Benfield, R. E.; Edwards, P. P.; Stacy, A. M. *J. Chem. Soc., Chem. Commun.* **1982**, 525–6. (b) Johnson, D. C.; Benfield, R. E.; Edwards, P. P.; Nelson, W. J. H.; Vargas, M. D. *Nature* **1985**, *314*, 231–5.

(13) (a) Pronk, B. J.; Brom, H. B.; de Jongh, L. J.; Longoni, G.; Ceriotti, A. *Solid State Commun.* **1986**, *59*, 349–54. (b) Teo, B. K.; DiSalvo, F. J.; Waszczak, J. V.; Longoni, G.; Ceriotti, A. *Inorg. Chem.* **1986**, *25*, 2262–5.

(14) Drake, S. R.; Edwards, P. P.; Johnson, B. F. G.; Lewis, J.; Marseglia, E. A.; Obertelli, S. D.; Pyper, N. C. *Chem. Phys. Lett.* **1987**, *139*, 336–44.

(15) Benfield, R. E. *Zeitschrift Physik* **1989**, *D12*, 453–5.

(7) Bullett, D. W. *Chem. Phys. Lett.* **1987**, *135*, 373–6.

(8) (a) Rösch, N.; Pacchioni, G. In *Clusters and Colloids: From Theory to Applications*; Schmid, G., Ed.; VCH: Weinheim, 1994; p 68. (b) Rösch, N.; Ackermann, L.; Pacchioni, G. *J. Am. Chem. Soc.* **1992**, *114*, 3549–55. (c) Rösch, N.; Ackermann, L.; Pacchioni, G.; Dunlap, B. I. *J. Chem. Phys.* **1991**, *95*, 7004–7. (d) Pacchioni, G.; Rösch, N. *Acc. Chem. Res.* **1995**, *28*, 390–7.

(9) Wooley, R. G. In *Transition Metal Clusters*; Johnson, B. F. G., Ed.; John Wiley & Sons: Chichester, 1980; p 649.

(10) Drake, S. R.; Johnson, B. F. G.; Lewis, J.; Wooley, R. G. *Inorg. Chem.* **1987**, *26*, 3952–6.

contrast, Curie-law behavior is not observed in the osmium system until ten metal atoms are present. If the Curie response is indicative of a mesometallic phase between molecular and bulk metallic behavior, its existence at a lower nuclearity for ruthenium suggests that ruthenium may approach metallic behavior faster than osmium. It would therefore seem logical to examine larger ruthenium clusters for the existence of mesometallic behavior and the onset of metallic character. However, studies with larger ruthenium clusters (comparable in size to those of the other metals above) have not been undertaken, possibly due to the lack of sufficiently high-yielding syntheses which permit detailed investigation of their physical properties.<sup>17</sup> We recently reported the preparation of  $[\text{Ru}_{10}(\mu\text{-H})(\mu_6\text{-C})(\text{CO})_{24}]^-$  (**1**)<sup>18</sup> and its substituted derivative  $[\text{Ru}_{10}(\mu\text{-H})(\mu_6\text{-C})(\text{CO})_{23}(\text{PPh}_3)]^-$  (**2**)<sup>18(a),19</sup> as their  $[\text{Ru}_2(\mu\text{-H})(\mu\text{-NC}_5\text{H}_4)_2(\text{CO})_4(\text{NC}_5\text{H}_5)_2]^+$  (**a**) salts in excellent yields and present herein an investigation of the EPR spectra of these clusters and magnetic susceptibility data for (**2a**), together with local density functional (LDF) computations on the isostructural dianion  $[\text{Ru}_{10}(\mu_6\text{-C})(\text{CO})_{24}]^{2-}$  (**6**) and its osmium analogue  $[\text{Os}_{10}(\mu_6\text{-C})(\text{CO})_{24}]^{2-}$  (**7**), the first such comparison of high-nuclearity clusters from the iron group, and the first to accurately reproduce the HOMO–LUMO energy gap obtained from electronic spectroscopy; these LDF studies further understanding of the approach to metallic behavior by rationalizing magnetic and spectroscopic data. This is the first report of EPR data from ruthenium clusters and the first investigation of the effects of ligand modification (phosphine substitution) and crystal packing on metal cluster EPR response. The electronic spectra of the decaruthenium cluster anion “family”,  $[\text{Ru}_{10}(\mu\text{-H})(\mu_6\text{-C})(\text{CO})_{24-x}(\text{PPh}_3)_x]^-$  ( $x = 0\text{--}4$ , **1–5**) and the dianion  $[\text{Ru}_{10}(\mu_6\text{-C})(\text{CO})_{24}]^{2-}$  (**6**)<sup>18(a)</sup> are also presented, the first study of the effects of ligand replacement on high-nuclearity cluster electronic spectra. In addition, diffuse reflectance solid-state electronic spectra of **2a** and **6d** are reported, the first such data for high-nuclearity carbonyl clusters.

## Experimental Section

**Syntheses.**  $[\text{Ru}_2(\mu\text{-H})(\mu\text{-NC}_5\text{H}_4)_2(\text{CO})_4(\text{NC}_5\text{H}_5)_2][\text{Ru}_{10}(\mu\text{-H})(\mu_6\text{-C})(\text{CO})_{24}]$  (**1a**),<sup>18</sup>  $[\text{Ru}_2(\mu\text{-H})(\mu\text{-NC}_5\text{H}_4)_2(\text{CO})_4(\text{NC}_5\text{H}_5)_2][\text{Ru}_{10}(\mu\text{-H})(\mu_6\text{-C})(\text{CO})_{23}(\text{PPh}_3)]$  (**2a**),  $[\text{PPh}_4][\text{Ru}_{10}(\mu\text{-H})(\mu_6\text{-C})(\text{CO})_{24-x}(\text{PPh}_3)_x]$  ( $x = 2\text{--}3$ , **3b–4b**),  $[\text{Ru}_2(\mu\text{-H})(\mu\text{-NC}_5\text{H}_4)_2(\text{CO})_4(\text{PPh}_3)_2][\text{Ru}_{10}(\mu\text{-H})(\mu_6\text{-C})(\text{CO})_{20}(\text{PPh}_3)_4]$  (**5c**),<sup>18(a),19</sup> and  $[\text{ppn}]_2[\text{Ru}_{10}(\mu_6\text{-C})(\text{CO})_{24}]$  (**6d**)<sup>18(a)</sup> were synthesized according to the literature.

**UV-vis-NIR Spectroscopy.** UV-vis-NIR spectra were recorded on a Perkin-Elmer Cary 5 spectrometer in the range 200–1400 nm using 0.1 cm cells against a solvent background. Solutions were made up in distilled  $\text{CH}_2\text{Cl}_2$ , typically in  $1.5\text{--}2.0 \times 10^{-4}$  M concentrations. Measurements were carried out on this initial concentration and remeasured after a 2/10 dilution. Solid-state UV-vis-NIR spectra were obtained using a Harrick “Praying Mantis” Diffuse Reflectance accessory and measured in the range 200–2000 nm.

**EPR Spectroscopy.** X-band EPR spectra of nitrogen-flushed polycrystalline samples or nitrogen-saturated acetone solutions (*ca.* 0.016 M) were recorded in derivative mode on a Bruker Instruments ESP 300E spectrometer, using 100 kHz modulation and 10 G modulation amplitude. Microwave frequency, power, and static field intensity were recorded automatically by the spectrometer. Temperatures of 5–65 K were attained with an Oxford Instruments ES9 helium

flow cryostat; an Oxford Instruments ITC4 temperature controller was employed. Spectral manipulation including deconvolution was accomplished using WIN-EPR software. The absence of a field dependence of the EPR responses indicates that no ferromagnetic impurities were present. Furthermore, ferromagnetic resonance lines can be quite sharp (<1 G) and saturate at low rf power levels,<sup>20</sup> in contrast to the broad, nonsaturable temperature-independent signals reported in this work.

Acetone solutions of **1a** were centrifuged in a Beckman L2-50 Ultracentrifuge by employing a SW40Ti rotor at 278 K and the following sequential cycles: 60 min at 25 000 rpm ( $\equiv 100\,000$  g), 30 min at 35 000 rpm ( $\equiv 200\,000$  g), and 30 min at 40 000 rpm ( $\equiv 285\,000$  g). Aliquots for frozen EPR investigation were taken from the top third of the centrifuged solution after each cycle.

**Magnetic Susceptibility.** Measurements were made on a polycrystalline sample of **2a** using a Quantum Design MPMS 5 Squid instrument operating under a field of 1 Tesla. A freshly prepared sample was rapidly weighed and transferred to a predried, preweighed, gelatin capsule in a nitrogen-filled glove-bag. The capsule was then rapidly weighed and transferred quickly, in a glove bag, to the center of the Squid instrument for evacuation and flushing with helium gas. The sample was checked for lack of decomposition after the measurements were completed.

The Squid instrument was calibrated by use of the accurately known magnetization value of a cylindrical sample of palladium, supplied by Quantum Design, and also by use of  $\text{CuSO}_4 \cdot 5\text{H}_2\text{O}$ . An error estimate in the measurement of magnetic susceptibility is  $\pm 10 \times 10^{-6} \text{ cm}^3 \text{ mol}^{-1}$ . The temperatures are accurate to  $\pm 0.1$  K. The diamagnetism of the gelatin capsule was corrected at all temperatures. The cluster molecular weight is 2559.5 and  $\chi_m$  (per mol) at all temperatures is  $+1384 \pm 10 \times 10^{-6} \text{ cm}^3 \text{ mol}^{-1}$  including diamagnetic corrections for valence electrons and  $+1016 \pm 10 \times 10^{-6} \text{ cm}^3 \text{ mol}^{-1}$  excluding correction for valence electrons of the decaruthenium cluster. Diamagnetic corrections were ( $\times 10^6 \text{ cm}^3 \text{ mol}^{-1}$ ) as follows:  $\text{Ru}^0$ ,  $-44$ ;  $\text{Ru}^{\text{VIII}}$ ,  $-7.2$ ; C,  $+5$ ; H,  $-2.93$ ; CO,  $-9.8$ ;  $\text{C}_5\text{H}_5\text{N}$ ,  $-49$ ;  $\text{C}_5\text{H}_4\text{N}$ ,  $-46.1$ ;  $\text{P}(\text{C}_6\text{H}_5)_3$ ,  $-167$ . Total diamagnetic correction per cluster (including valence electrons) =  $-1150 \times 10^{-6} \text{ cm}^3 \text{ mol}^{-1}$ , and total diamagnetic correction per cluster (excluding valence electrons) =  $-782 \times 10^{-6} \text{ cm}^3 \text{ mol}^{-1}$ .

**Local Density Calculations.** All calculations reported in this work were performed using the Amsterdam Density Functional (ADF) Package (Version 2.0.1) of Baerends *et al.*<sup>21</sup> The molecular orbitals were expanded in a triple- $\zeta$  STO basis for Ru or Os and a double- $\zeta$  basis for C and O.<sup>22</sup> Core orbitals (1s for C, O; 1s-4p for Ru; 1s-5p for Os) were kept frozen throughout. The local spin density (LSD) exchange potential was used,<sup>23</sup> along with the Vosko–Wilk–Nusair approximation to the correlation energy.<sup>24</sup> Molecular geometries were taken from the crystal structures of **6**<sup>25</sup> and **7**,<sup>26</sup> idealized to  $D_{2d}$  symmetry. Metal–metal bond lengths within the octahedral core were set to 2.86 Å and all others to 2.77 Å, in accord with the available crystallographic data. All M–CO bond lengths were set to 1.86 Å, and all C–O bonds set to 1.15 Å.

## Results and Discussion

**Ground-State Electronic Structure.** Results from the LDF study are presented first and are then applied as an aid in the interpretation of the optical spectra. A comparison of the

(19) Cifuentes, M. P.; Humphrey, M. G.; Skelton, B. W.; White, A. H. *Organometallics* **1995**, *14*, 1536–8.

(20) Kittel, C. *Introduction to Solid State Physics*; John Wiley: New York, 1966.

(21) (a) Baerends, E. J.; Ellis, D. E.; Ros, P. *Chem. Phys.* **1973**, *2*, 42–51. (b) Baerends, E. J.; Ros, P. *Chem. Phys.* **1973**, *2*, 52–9. (c) Baerends, E. J.; Ros, P. *Int. J. Quantum Chem.* **1978**, *S12*, 169–90.

(22) Vernooijs, P.; Snijders, G. L.; Baerends, E. J. *Slater Type Basis Functions for the Whole Periodic Table*; Internal Report, Vrije Universiteit: Amsterdam, 1981.

(23) Ziegler, T. *Chem. Rev.* **1991**, *91*, 651–77.

(24) Vosko, S. H.; Wilk, L.; Nusair, M. *Can. J. Phys.* **1980**, *58*, 1200–11.

(25) Chihara, T.; Komoto, R.; Kobayashi, K.; Yamazaki, H.; Matsuura, Y. *Inorg. Chem.* **1989**, *28*, 964–7.

(26) Jackson, P. F.; Johnson, B. F. G.; Lewis, J.; McPartlin, M.; Nelson, W. J. *J. Chem. Soc., Chem. Commun.* **1980**, 224–6.

(16) de Aguiar, J. A. O.; Mees, A.; Darriet, J.; de Jongh, L. J.; Drake, S. R.; Edwards, P. P.; Johnson, B. F. G.; Lewis, J. *Solid State Commun.* **1988**, *66*, 913–6.

(17) Cifuentes, M. P.; Humphrey, M. G. In *Comprehensive Organometallic Chemistry II*; Abel, E. W., Stone, F. G. A., Wilkinson, G., Eds.; Elsevier: Oxford, 1995; Vol. 7, Chapter 16, pp 909–62.

(18) (a) Cifuentes, M. P.; Humphrey, M. G.; Skelton, B. W.; White, A. H. *J. Organomet. Chem.* **1996**, *507*, 163–78. (b) Cifuentes, M. P.; Humphrey, M. G.; Skelton, B. W.; White, A. H. *Organometallics* **1993**, *12*, 4272–4.

**Table 1.** UV-vis Spectral Data for **1–6** and **7d**

complex <sup>f</sup>																						
<b>1a</b>			<b>2a</b>			<b>3b</b>			<b>4b</b>			<b>5c</b>			<b>6d</b>			<b>7d<sup>d</sup></b>				
$\lambda^a$	$\epsilon$	$\Delta E^c$	$\lambda^a$	$\epsilon$	$\Delta E^c$	$\lambda^a$	$\epsilon$	$\Delta E^c$	$\lambda^a$	$\epsilon$	$\Delta E^c$	$\lambda^a$	$\epsilon$	$\Delta E^c$	$\lambda^a$	$\epsilon$	$\Delta E^c$	$\lambda^a$	$\epsilon$	$\Delta E^c$		
234	101 300	5.29	236	95 600	5.25	234	158 000	5.31	232	146 100	5.34	232	137 500	5.34	232	133 200	5.34	230	11 000	5.39		
257	114 400	4.82	257	100 200	4.82	260	113 000	4.76	261	97 900	4.75	264	91 800	4.70	261	83 400	4.75	312	1 740	3.98		
									268	95 200	4.63											
									275	87 000	4.49											
381	23 100	3.26	381 sh <sup>e</sup>			360	44 100	3.44							384	19 200	3.22	385	800	3.22		
			406	26 100	3.05	417	37 200	2.98	424	36 200	2.93	432	28 700	2.88	470	10 400	2.64	482	1 250	2.57		
570	8 300	2.18	569	10 400	2.18	580	15 900	2.14	590	16 400	2.10	599	13 800	2.07	590	6 500	2.10	662	90	1.87		
725	5 100	1.71	732	7 300	1.69	706	10 500	1.76	709	8 300	1.75				729	4 500	1.72	771	60	1.61		
1020		1.21	1020		1.21	1020		1.21	1020		1.21	1020		1.21	1020		1.21	830		1.51		

<sup>a</sup> All wavelengths in nm,  $\pm 1$  nm. <sup>b</sup> Errors in extinction coefficients ca.  $\pm 10\%$ . <sup>c</sup>  $\Delta E$  in eV. <sup>d</sup> Reference 10. <sup>e</sup> sh, shoulder. <sup>f</sup> **a**, **b**, **c**, and **d** refer to complexes with  $[\text{Ru}_2(\mu\text{-H})(\mu\text{-NC}_5\text{H}_4)_2(\text{CO})_4(\text{NC}_5\text{H}_5)_2]^+$ ,  $[\text{PPh}_4]^+$ ,  $[\text{Ru}_2(\mu\text{-H})(\mu\text{-NC}_5\text{H}_4)_2(\text{CO})_4(\text{PPh}_3)_2]^+$ , and  $[\text{ppn}]$  cations, respectively.

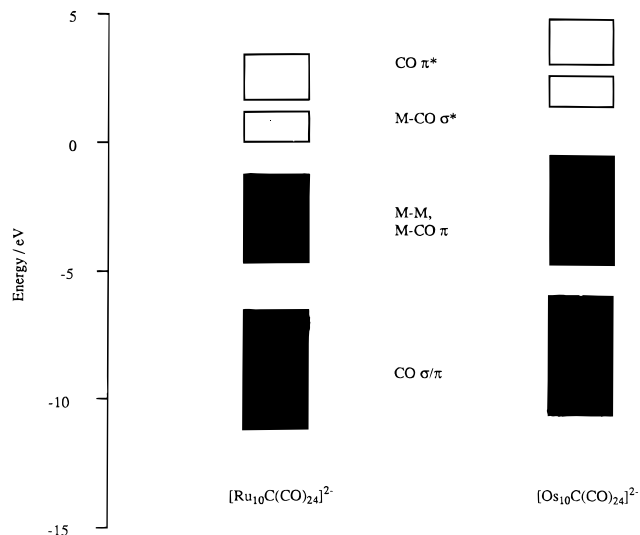


**Figure 2.** Frontier orbital regions of  $[\text{Ru}_{10}(\mu_6\text{-C})(\text{CO})_{24}]^{2-}$  (**6**) and  $[\text{Os}_{10}(\mu_6\text{-C})(\text{CO})_{24}]^{2-}$  (**7**).

frontier orbital regions of **6** and **7** is illustrated in Figure 2. In both cases, there is a broad band consisting of the occupied CO  $2\sigma$ ,  $3\sigma$ , and  $1\pi$  orbitals between  $-11$  and  $-7$  eV, followed by a band of metal-based levels between  $-5$  and  $-1.2$  eV (Ru) and  $-5$  and  $-0.7$  eV (Os). The unoccupied manifold consists of a series of M–CO antibonding levels, with a band of CO  $\pi^*$  orbitals at higher energy. The most significant difference between the two systems is the smaller HOMO–LUMO gap in the ruthenium cluster (1.07 eV compared to 1.27 eV in the osmium cluster). The reason for this difference can be traced to the nature of the metal–CO bonding in the HOMO and LUMO, contour plots of which are shown in Figure 3. The plots are shown in a plane containing  $\text{Ru}_{1-4}$ . The figures indicate that the HOMO is M–CO  $\pi$  bonding, whereas the LUMO has M–CO  $\sigma$  antibonding character. The bonding situation therefore resembles that in simple mononuclear metal carbonyl complexes, where the HOMO is stabilized by metal–ligand backbonding, whereas the LUMO is destabilized by interactions with the CO  $\sigma$  lone pair orbital. In general, it is found that the back-bonding contribution is greater in complexes of the third transition series than in second transition series analogues, due to the higher energy and greater radial extent of the 5d orbitals relative to 4d resulting in a larger HOMO–LUMO gap for the 5d metal complexes. The differences between 4d and 5d atomic orbitals are clearly transmitted to the cluster compounds, resulting in a smaller HOMO–LUMO gap in the ruthenium system. In contrast to the present study, the only previous report of LDF calculations on large iron group clusters found a HOMO–LUMO energy gap of 0.5 eV in **7**;<sup>7</sup>

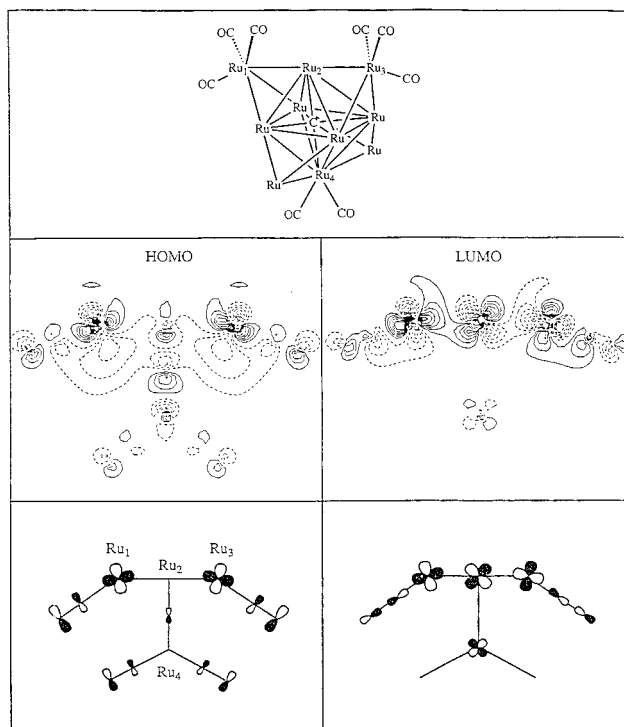


**Figure 3.** Contour plots of the HOMO and LUMO of  $[\text{Ru}_{10}(\mu_6\text{-C})(\text{CO})_{24}]^{2-}$  (**6**).

the result from the current work (1.3 eV) is in much closer agreement with the spectroscopically-obtained  $\lambda_{\text{onset}}$  (1.5 eV; see below).

**UV-vis-NIR Spectra.** There have been few reports of electronic spectra of high-nuclearity clusters (in particular, there has been no systematic comparison of the effect of ligand variation thus far). The spectra of  $[\text{Ru}_{10}(\mu\text{-H})(\mu_6\text{-C})(\text{CO})_{24}]^-$  (**1a**) and the series of triphenylphosphine derivatives **2a–5c**, together with that of the cluster dianion  $[\text{ppn}]_2[\text{Ru}_{10}(\mu_6\text{-C})(\text{CO})_{24}]^{2-}$  (**6d**) were consequently recorded; important data are presented in Table 1, together with the previously reported data for  $[\text{ppn}]_2[\text{Os}_{10}(\mu_6\text{-C})(\text{CO})_{24}]^{2-}$  (**7d**).<sup>10</sup> All the spectra are broadly similar to that of the decaosmium cluster dianion, with intense high energy and weaker low energy absorptions, and with four to five peaks superimposed on a continuous absorption from 200 to 1000 nm. The large number of electric dipole-allowed transitions in these clusters prohibits a detailed assignment of the observed electronic spectra, but it is possible to draw some qualitative conclusions from the orbital energies shown in Figure 2.

Comparison across the series of decaruthenium complexes **1a–6d**, and with data from **7**, reveals some trends.

(a) The decaruthenium clusters have intense absorptions, similar to the osmium dianion, at about 235 nm ( $\Delta E \approx 5.3$  eV); the separation of metal and CO  $\pi^*$  bands is consistent with the assignment of this intense feature as a  $M-M^* \rightarrow CO\ 2\pi^*$  transition.

(b) The decaruthenium clusters have a distinct absorption at about 260 nm ( $\Delta E \approx 4.8$  eV), possibly present as a shoulder in the osmium cluster, although it was not identified as such.

(c) The osmium cluster has a small peak at 385 nm ( $\Delta E \approx 3.2$  eV); in the ruthenium analogue, it appears almost unchanged at 384 nm, but its position seems strongly dependent on the ligand environment of the anionic cluster, moving to 360 nm ( $\Delta E \approx 3.4$  eV) on bis(phosphine) substitution and being submerged by the intense high frequency band on further substitution.

(d) Similarly, the positions of the lower energy bands also seem to be ligand dependent, with the band at 570 nm ( $\Delta E \approx 2.2$  eV) in the unsubstituted cluster moving to lower energy on increasing phosphine ligation.

(e) The lowest energy bands show a strong metal dependence. The absorption in **7** is reported to extend to 830 nm ( $\Delta E \approx 1.5$  eV),<sup>6</sup> whereas the onset wavelength in the decaruthenium clusters is at much lower energy ( $\lambda_{\text{onset}} \approx 1020$  nm, corresponding to  $\Delta E \approx 1.2$  eV) with no ligand dependence; the difference in HOMO–LUMO gaps between the two clusters (0.2 eV) correlates well with the observed difference in onset energies (0.3 eV).

(f) The intensity of the ruthenium absorptions are an order of magnitude greater than the analogous reported osmium values.<sup>10</sup>

High-nuclearity clusters are of interest because of their position as potential intermediate species in the transition from molecular to metallic behavior; as such, it is of importance to compare their physical properties with those of metal particles. The UV-visible absorption spectra for a 10 nm diameter colloid particle of ruthenium has been calculated using Mie theory.<sup>27</sup> As with most colloidal metallic elements in this very small particle size domain, there is only a continuous absorption in the visible range, rising to broad and poorly resolved absorption bands in the ultraviolet region near 200 nm; it should be emphasized that within the 3–20 nm diameter size range typical for chemically produced colloids, there is not a strong dependence of absorption spectra on particle size. The decaruthenium clusters described in this work are ligated metal particles of almost 1 nm diameter. Although for particles smaller than about 3 nm it becomes necessary to correct for restrictions in the mean-free path of conduction electrons, the effect is only to broaden and decrease the height of absorption bands and not to shift absorption maxima. The spectrum of a less free-electron metal such as ruthenium has considerable interband character, with an inflexion in the absorption spectrum at about 450 nm. Comparison of this featureless spectrum with the better-defined spectra of the decaruthenium clusters above shows not only that the latter contain fine structure which can be tentatively assigned to the particular transitions discussed above but also that the spectra appear to be beginning to take on the character of slightly larger metal particles with strong absorption at high energy, broad absorption to low energy, and interband transitions.

**Diffuse Reflectance UV-vis-NIR Spectra.** Very few solid-state electronic spectra of metal clusters have been reported, with almost all previous papers dealing with solution spectra.<sup>6</sup> The spectra of  $[\text{Au}_{55}(\text{PPh}_3)_{12}\text{Cl}_6]$  (**8**) in the solid state and solution are reported to differ substantially;<sup>6</sup> on dilution, the

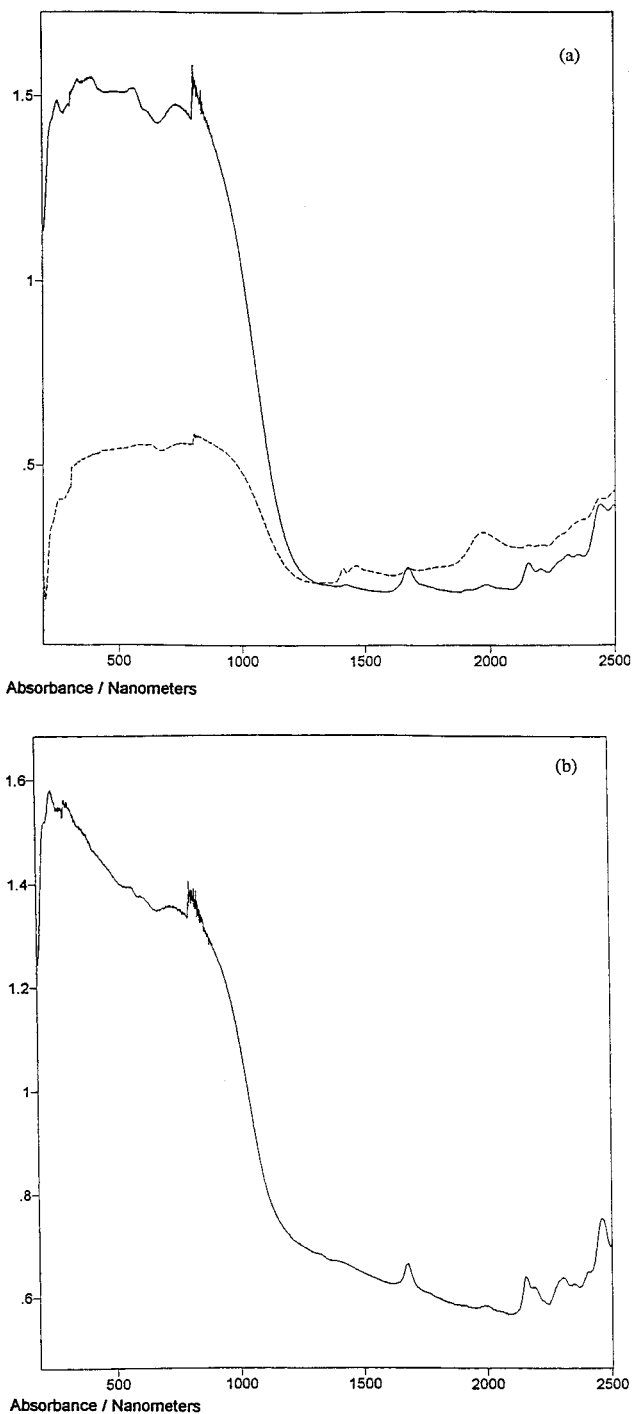


**Figure 4.** Diffuse reflectance UV-vis-NIR spectra of (a)  $[\text{Ru}_2(\mu\text{-H})-(\mu\text{-NC}_5\text{H}_4)_2(\text{CO})_4(\text{NC}_5\text{H}_5)_2][\text{Ru}_{10}(\mu\text{-H})(\mu_6\text{-C})(\text{CO})_{23}(\text{PPh}_3)]$  (**2a**) (—) shows the effect of dilution and (b)  $[\text{ppn}]_2[\text{Ru}_{10}(\mu\text{-H})(\mu_6\text{-C})(\text{CO})_{24}]$  (**6d**).

former took on the characteristics of the latter (an unusual observation since a decrease in relative intensity without spectral modification would be predicted). The major difference (notably, a very broad, intense absorption,  $\lambda_{\text{max}} \approx 500$  nm, and extending to 2000 nm) was assigned to charge transfer between clusters in the solid state; in this regard, it is perhaps significant that **8** is an odd-electron cluster. Diffuse reflectance UV-vis-NIR spectra of the even-electron clusters  $[\text{Ru}_2(\mu\text{-H})(\mu\text{-NC}_5\text{H}_4)_2(\text{CO})_4(\text{NC}_5\text{H}_5)_2][\text{Ru}_{10}(\mu\text{-H})(\mu_6\text{-C})(\text{CO})_{23}(\text{PPh}_3)]$  (**2a**) and  $[\text{ppn}]_2[\text{Ru}_{10}(\mu_6\text{-C})(\text{CO})_{24}]$  (**6d**) were obtained and are shown in Figure 4. As with the  $\text{Au}_{55}$  cluster, a very broad absorption is observed, extending to a  $\lambda_{\text{onset}}$  at around 1300 nm, considerably lower in energy than for the solution spectra, with a slight shift to lower

(27) Creighton, J. A.; Eadon, D. G. *J. Chem. Soc., Faraday Trans.* **1991**, *87*, 3881–91.

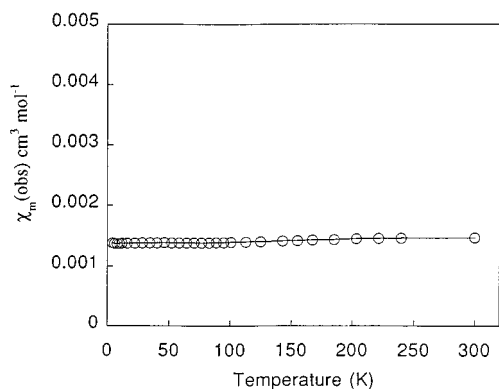


**Figure 5.** Temperature dependence of molar magnetic susceptibility of  $[\text{Ru}_2(\mu\text{-H})(\mu\text{-NC}_5\text{H}_4)_2(\text{CO})_4(\text{NC}_5\text{H}_5)_2][\text{Ru}_{10}(\mu\text{-H})(\mu_6\text{-C})(\text{CO})_{23}(\text{PPh}_3)]$  (**2a**). This value of  $\chi_m$  includes a diamagnetic correction for all ruthenium valence electrons. The value of  $\chi_m$  excluding the valence electrons on the decaruthenium anionic clusters is  $+1016 \times 10^{-6} \text{ cm}^3 \text{ mol}^{-1}$  or  $+1124 \times 10^{-6} \text{ cm}^3 \text{ mol}^{-1}$ , depending on the value used for ruthenium; see the Results and Discussion and ref 29b.

energy on moving from the dianion to the phosphine-substituted monoanion cluster. Superimposed on the broad absorption is fine structure with absorption maxima corresponding to those in the solution spectra; unlike **8**, dilution of the sample of **2a** with  $\text{CaCO}_3$  did not lead to the solid-state spectrum acquiring the appearance of the solution spectrum. For **2a**, bands at around 1660 nm are assigned to second overtones of carbonyl stretching frequencies; first overtones are also evident at around 2400 nm.

**Magnetic Susceptibility.** The magnetic susceptibility of **2a** was determined over the range 4.2–300 K (Figure 5). The temperature independent molecular susceptibility  $\chi_m = +1384 \pm 10 \times 10^{-6} \text{ cm}^3 \text{ mol}^{-1}$  is significantly higher than those for related osmium clusters (for example,  $\chi_m$  for  $[\text{H}_2\text{Os}_{10}\text{C}(\text{CO})_{24}]$  (**9**) is  $+326 \pm 30 \times 10^{-6} \text{ cm}^3 \text{ mol}^{-1}$  over the range 150–298 K). In both of these cases, the diamagnetic correction for all valence electrons on ruthenium and osmium were included in the  $\chi_m$  calculation. The magnetic susceptibility of several lower nuclearity ruthenium clusters has been reported previously;<sup>16</sup> all examples other than  $[\text{Ru}_3(\text{CO})_{12}]$  (**10**), namely  $[\text{H}_2\text{Ru}_4(\text{CO})_{13}]$  (**11**),  $[\text{Ru}_5(\mu_5\text{-C})(\text{CO})_{15}]$  (**12**),  $[\text{Ru}_6(\mu_6\text{-C})(\text{CO})_{17}]$  (**13**), and  $[\text{ppn}]_2[\text{Ru}_6(\text{CO})_{18}]$  (**14d**), contained both temperature independent and temperature dependent contributions. The temperature independent  $\chi_0$  contributions were not corrected for the diamagnetism of the metal atoms, with  $\chi_0$  values of 300 (**10**), 500 (**11**), 750 (**12**), 1000 (**13**), and 4000 (**14d**) (all  $\times 10^{-6} \text{ cm}^3 \text{ mol}^{-1}$ ); following the same procedure, the susceptibility  $\chi_0$  for **2a** would be  $+944 \times 10^{-6} \text{ cm}^3 \text{ mol}^{-1}$  (where diamagnetic correction has been applied for the two ruthenium atoms present in the cation but not for the ten cluster core ruthenium atoms). Although correction procedures and diamagnetic susceptibility correction per ligand may vary between the two previous reports and the current work, in all cases a small net positive temperature independent term, ascribed to a combination of orbital diamagnetic and Van Vleck contributions, results. As Van Vleck temperature-independent paramagnetism is inversely related to the energy gap between the occupied and unoccupied states, which decreases with increasing nuclearity, it is not surprising that a gradual increase in  $\chi_0$  with increasing nuclearity is observed.<sup>13(b)</sup> It has recently been pointed out, however, that evidence for growing Van Vleck paramagnetism as a function of cluster size with a series of osmium clusters of varying nuclearity is a result of the correction employed; all the electrons of the osmium metal atoms were factored into the correction, including the valence electrons. It is appropriate to correct only

for the diamagnetism of the core electrons, if the behavior of the valence electrons in the cluster is to be assessed, clearly essential in probing the development of metallic character. With the latter correction applied, the susceptibility as a function of cluster size for the osmium clusters is found to fluctuate around zero.<sup>31</sup> Correcting the data from **2a** for the diamagnetism of the two ruthenium atoms in the cation and for the core electrons of the ten cluster ruthenium atoms results in a susceptibility of  $+1016 \pm 10 \times 10^{-6} \text{ cm}^3 \text{ mol}^{-1}$ . Following this procedure, susceptibilities for the ruthenium clusters investigated previously are  $+329$  (**10**),  $+532$  (**11**),  $+778$  (**12**),  $+1035$  (**13**), and  $+4048$  (**14**) (all  $\times 10^{-6} \text{ cm}^3 \text{ mol}^{-1}$ ). In these corrections, the value for  $\text{Ru}^{\text{VIII}}$  of  $-7.2 \times 10^{-6} \text{ cm}^3 \text{ mol}^{-1}$  was estimated from the literature value for  $\text{Ru}^{\text{VII}}$ ,<sup>32</sup> by analogy to the values given for  $\text{Os}^{\text{VIII}}$  and  $\text{Os}^{\text{VII}}$ . The recent calculations by van Ruitenbeek<sup>29(b)</sup> for the osmium clusters resulted in a value of  $-26 \times 10^{-6} \text{ cm}^3 \text{ mol}^{-1}$  per osmium excluding the valence electrons, which compares with  $-11 \times 10^{-6} \text{ cm}^3 \text{ mol}^{-1}$  for  $\text{Os}^{\text{VIII}}$  given by Königs tables. A value per ruthenium of *ca.*  $-18 \times 10^{-6} \text{ cm}^3 \text{ mol}^{-1}$  might thus be more appropriate here. This would lead to a total diamagnetic correction for **2a** of  $-890 \times 10^{-6} \text{ cm}^3 \text{ mol}^{-1}$  and a  $\chi_m$  value of  $+1124 \pm 10 \times 10^{-6} \text{ cm}^3 \text{ mol}^{-1}$ . Likewise, the  $\chi_m$  values for the other ruthenium clusters are  $+361$  (**10**),  $+575$  (**11**),  $+832$  (**12**),  $+1099$  (**13**), and  $+4114$  (**14**). In all these calculations, a trend of increasing  $\chi_0$  with increasing nuclearity is observed, in contrast to the above-mentioned data for osmium clusters.

**EPR Spectra.** Results of EPR spectroscopy studies on polycrystalline solid samples of **1a** and **2a** are shown in Table 2 together with the previously reported data for the isostructural osmium analogue  $[\text{H}_2\text{Os}_{10}\text{C}(\text{CO})_{24}]$  (**9**)<sup>3</sup> for comparison. Temperature dependence and power saturation studies of **1a** are shown in Figure 6. The temperature-independent intensities observed with **1a** are in contrast to all previous reports of EPR studies of ligated metal clusters, which show temperature-dependent (Curie) responses. Similarly, our inability to saturate the signal contrasts with previous EPR reports on cluster complexes, where the signals were saturable. Although we were unable to determine a spin–lattice relaxation time  $T_1$ , the spin–spin relaxation time  $T_2$  for **1a** is  $1.8 \times 10^{-10} \text{ s}$  at 5 K, comparable to that of the isostructural osmium analogue **9** ( $10^{-9} \text{ s}$ ) and orders of magnitude slower than bulk metal (for example, osmium is  $5 \times 10^{-15} \text{ s}$ ).<sup>3</sup> The line shape of metal particles smaller than the microwave skin depth (as this cluster is) do not show the asymmetric Dysonian shape characteristic of thicker samples, but their symmetric Lorentzian forms are reported to tend to Dysonian at low temperature;<sup>3</sup> the symmetric line shape for **1a** becomes somewhat more asymmetric on decreasing the temperature from 60 K ( $A/B = 0.83$ ) to 5 K ( $A/B = 0.71$ ). The temperature dependence of intensity and line shape and power saturation behavior are similar to those of bulk metal, but the spin–spin relaxation rate is substantially slower.

As mentioned above, previously reported EPR studies with medium- to high-nuclearity carbonyl clusters have only shown

(28) Figgis, B. N. *Introduction to Ligand Fields*; Interscience: New York, 1966.

(29) (a) van Ruitenbeek, J. M.; van Leeuwen, D. A. *Phys. Rev. Lett.* **1991**, *67*, 640–3. (b) van Ruitenbeek, J. M. *Zeitschrift Physik* **1991**, *D19*, 247–50.

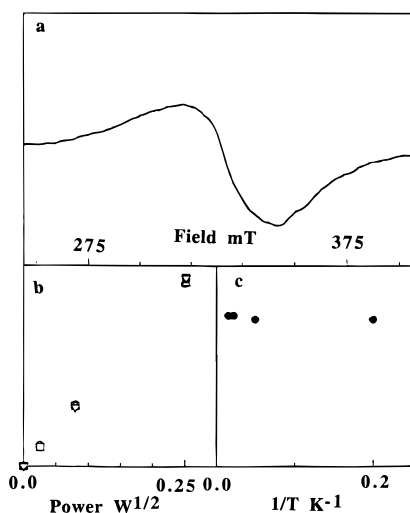
(30) Pace, R. J.; Smith, P.; Bramley, R.; Stehlik, D. *Biochim. Biophys.* **1991**, *1058*, 161–70.

(31) van Ruitenbeek, J. M.; van Leeuwen, D. A.; de Jongh, L. J. In *Physics and Chemistry of Metal Cluster Compounds*; de Jongh, L. J., Ed.; Kluwer: Dordrecht, The Netherlands, 1994; pp 277–306.

(32) *Landolt-Bornstein: Numerical Data and Functional Relationships in Science and Technology*; Bortfeld, J., Kramer, B., Eds; Springer: Berlin, 1991.

**Table 2.** Results of X-band Spectra on Polycrystalline Samples of **1a** and **2a** (This Work) and **9<sup>a</sup>**

	(1)	(2)	9 <sup>a</sup>
EPR signal	one component	two components	one component
EPR intensity	<i>T</i> independent	<i>T</i> independent	<i>T</i> dependent (20–100 K)
isotropic <i>g</i> value	2.045(3)	2.053(2)	2.280
$\Delta H_{pp}$	285 G (60 K) 350 G (5 K)	445(10) G	38(1) G (20 K)
<i>T</i> <sub>1</sub> (s)	not determined	10 <sup>-4</sup> (10 K)	10 <sup>-3</sup> (12 K)
<i>T</i> <sub>2</sub> (s)	1.8 × 10 <sup>-10</sup>	10 <sup>-10</sup> (10 K)	10 <sup>-9</sup> (20 K)
saturable signal	no	yes	yes
<i>P</i> <sub>1/2</sub>		0.74 mW (5 K)	not reported

<sup>a</sup> Reference 3.

**Figure 6.** (a) X band line shape for  $[\text{Ru}_2(\mu\text{-H})(\mu\text{-NC}_5\text{H}_4)_2(\text{CO})_4(\text{NC}_5\text{H}_5)_2][\text{Ru}_{10}(\mu\text{-H})(\mu_6\text{-C})(\text{CO})_{24}]$  (**1a**). Spectrometer settings: microwave frequency, 9.425 GHz; microwave power, 20  $\mu\text{W}$ ; temperature, 5 K. (b) Microwave power saturation plot (as per ref 30) for **1a**. Temperatures 5 K ( $\Delta$ ), 20 K ( $\circ$ ), 42 K ( $\square$ ), 63 K ( $\nabla$ ). Signal does not saturate at any of these temperatures. (c) Temperature dependence of signal intensity for **1a** measured at 63.3 mW microwave power. No transition to Curie-type behavior is observed at 5 K.

Curie behavior, assigned variously to a mesometallic regime between molecular and bulk metal<sup>3</sup> or to a variety of possible contaminations (surface oxidation, variable stoichiometry of hydride ligands, positional isomerism of ferromagnetic and non-ferromagnetic metals).<sup>5(b)</sup> As there have been no previous reports of temperature-independent EPR signals from clusters, we have examined possible sources of the temperature-independent response, namely solid-state effects (perhaps weak conduction through the solid, mediated by either anion packing or the diruthenium cation), surface oxidation of crystalline material, or the presence of small metal particles or colloids (possibly due to cluster decomposition).

The decaruthenium anions in **1a** form apex-to-base linked piles in the crystal lattice (ref 18a); conduction through the anion piles is clearly possible. To investigate whether this packing motif is responsible for the EPR signal above, the phosphine-substituted derivative **2a** was examined; the bulky phosphine

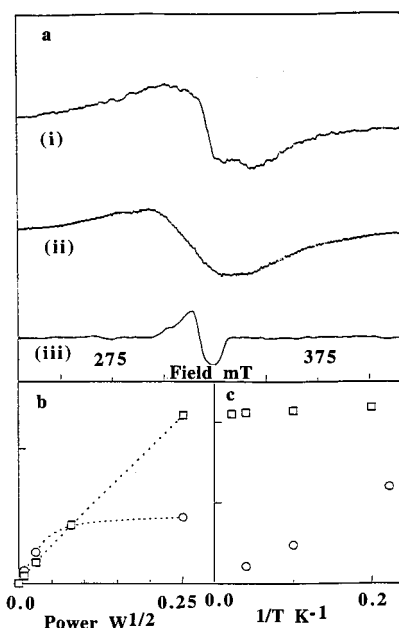


**Figure 7.** (a) (i) X band line shape for **2a**. Spectrometer settings: microwave frequency, 9.425 GHz; microwave power, 20  $\mu\text{W}$ ; temperature, 10 K. (ii) and (iii) Signal deconvolution using Figure 1 as the shape function for a cubic spline, to subtract the line shape of the temperature independent component (ii) and afford the signal shape of the Curie component (iii). (b) Microwave power saturation plot at 10 K for line shape component: (a) (ii) ( $\square$ ) and (a) (iii) ( $\circ$ ). (c) Temperature dependence of signal intensity for line shape components: (a) (ii) ( $\square$ ) (showing temperature independent behavior) and for (a) (iii) ( $\circ$ ) (showing Curie response).

ligand disrupts the columnar anion packing.<sup>18(a)</sup> The EPR signal for **2a** consists of two deconvolutable components (Figure 7), one of which parallels the behavior of the unsubstituted cluster **1a**. The other component shows Curie-type dependence, has a much smaller  $\Delta H_{pp}$ , and is saturable; this signal is similar to responses observed with medium- to high-nuclearity clusters of other metals, the origin of which is also uncertain. The temperature-independent component of **2a** suggests that crystal packing is not the source of the unusual EPR signal in **1a** and that **1a** is not unique in its behavior. To probe the generality of the temperature-independent response in cubic-close-packed

decaruthenium cluster cores, we have investigated the EPR of  $[\text{PPh}_4]_2[\text{Ru}_{10}(\mu_6\text{-C})(\text{CO})_{24}]$  (**6d**), which (like **2a**) consists of two components. We have not been able to deconvolute the components satisfactorily; however, one has been identified as temperature-independent and not saturable. Cluster **6d** has an organic cation, and the temperature-independent response of one of its EPR components eliminates mediation by the diruthenium cation as the origin of the unusual signal.

Unlike the mixed-metal nickel-platinum clusters examined recently by van Leeuwen *et al.*<sup>5(b)</sup> the decaruthenium clusters, which are the subject of our studies, have well-defined numbers of hydride ligands (clusters **1a** and **2a** have one each, the location of which has been shown, crystallographically in **1a** and spectroscopically in **2a**, to be external to the metal core) and cannot show positional isomerism of metals (as they are homometallic). We have also examined decomposed samples of these clusters (several months old), and they are EPR-silent, indicating that oxidation or decomposition products of **1a** are not responsible, although metastable oxidation/decomposition products are not excluded. To prove definitively that the observed signals are intra- rather than intermolecular in origin, we have examined the frozen solution EPR of **1a** (responses arising from solid-state mediation will not be observed under these conditions); the EPR spectrum of an acetone solution of **1a** (0.016 M, 12 K) still shows the temperature-independent signal, providing further evidence that intercluster effects are not the source of the temperature-independent behavior. To exclude colloidal metal/metal particulates or metal oxide particles as the origin of the temperature-independent behavior, an acetone solution of **1a** was centrifuged at successively higher speeds, and the frozen solution EPR spectrum was measured for aliquots obtained after each centrifuge run; the spectra after each run are identical to that of the frozen solution before centrifugation. Under these conditions, contaminants as above would be removed from suspension in the solution during the third centrifugation unless their radii are less than about 8 Å (for a particle of the density of bulk ruthenium metal). As the smallest metal particles in metal colloids have  $10^3$ – $10^4$  atoms,<sup>4</sup> corresponding to a particle of radius at least 14 Å, and metal particles and metal oxide particles are larger, it seems that these can be excluded from consideration as the source of the observed response. To summarize, the studies above excluded solid-state packing (by investigation of decaruthenium systems with differing packing characteristics), the unusual diruthenium cation (by replacement with  $[\text{PPh}_4]^+$ ), and metal colloids, particles, and oxides (by examining frozen centrifuged solutions) as the source of the unprecedented temperature-independent EPR signals. Furthermore, these clusters have stoichiometrically precise numbers of hydride ligands. This evidence suggests that the decaruthenium clusters are responsible for the temperature-independent signal.

**Discussion.** The foci of the present studies are to shed light on the transition from molecular to metallic behavior which should ensue upon increasing cluster nuclearity, to probe the possible intermediacy of a mesometallic phase and, if possible, to clarify uncertainties from previous studies regarding unusual magnetic behavior. Despite some similarities to metallic properties, the present study has afforded data consistent with (carbido)decametallc carbonyl clusters and related ligated clusters possessing molecular rather than mesometallic character. The electronic spectra contain broad absorptions extending from the UV through to the visible and into the near IR region similar to that of colloidal metal particles but with distinct maxima superimposed. The LDF calculations have indicated the origin of some of the transitions in the electronic spectra and confirmed

that a substantial HOMO–LUMO energy gap, much too large for metallic behavior, exists in these clusters.

The magnetic susceptibility data reveal a small, positive, temperature independent contribution arising from orbital diamagnetic and Van Vleck origins, a result expected for a small diamagnetic multimetallic cluster complex. This temperature independent paramagnetism is not the Pauli paramagnetism of the bulk metal; the LDF studies indicate that the density of states in these clusters is not sufficient to sustain metallic magnetic behavior. A quasicontinuous density of orbital levels is required in the vicinity of the HOMO (or Fermi level) for the temperature-independent electronic susceptibility  $\chi_e$  characteristic of a metal. The calculated orbital energies from the LDF calculations provide a rationale for the observed Van Vleck magnetic response of **2a**. The lowest energy one-electron excitation involving the metal-based HOMO-LUMO levels gives rise to an excited  $(t_2)^5(t_1)^1$  configuration, assuming parent  $T_d$  symmetry for the decaruthenium cluster. The excited spin-singlet states arising from this configuration are therefore of  $A_2$ ,  $E$ ,  $T_1$ , and  $T_2$  symmetry. The energy range of these states is expected to be small due to the large reduction in interelectron repulsion as discussed above. The orbitally degenerate  $^1T_1$  state can be directly mixed into the  $^1A_1$  ground state through a second-order Zeeman effect<sup>28</sup> and, given that this state could well lie below  $10\,000\text{ cm}^{-1}$ , will give rise to a significant TIP term. In addition, higher order processes will mix the degenerate  $^1T_2$  state into the ground state as well. A number of other orbitally degenerate states lie to higher energy, and these too will contribute to the ground state TIP. Consequently, given the low energy of at least two of the orbitally degenerate excited states as well as the large number of such states, it is not surprising that the TIP contribution is moderately large. In contrast to previous studies of smaller ruthenium clusters and osmium clusters of a similar size, we find no evidence for temperature dependent susceptibility; our results are consistent with the recent single crystal studies of nickel and nickel-platinum clusters.<sup>5(b)</sup> Although we cannot comment definitively on the Curie behavior of the osmium clusters, the lack of Pauli paramagnetism or a temperature dependent susceptibility for **2a** is consistent with the suggestion of van Leeuwen *et al.* that impurities (perhaps particle surface contamination), rather than mesometallic behavior, are responsible for the temperature dependent results of the earlier work. The LDF calculations are consistent with an adventitious origin of the temperature dependent paramagnetism.

It has been suggested previously that the small HOMO–LUMO gap in large metal clusters may lead to a high-spin ground state, as it does for mononuclear systems with similar frontier orbital separations,<sup>6</sup> which would result in the Curie paramagnetism observed with the decaosmium cluster **7** and lower nuclearity ruthenium clusters **11**–**14**. In order to investigate this possibility, the energy of the lowest lying triplet state has been calculated for both  $[\text{Ru}_{10}(\mu_6\text{-C})(\text{CO})_{24}]^{2-}$  (**6**) and  $[\text{Os}_{10}(\mu_6\text{-C})(\text{CO})_{24}]^{2-}$  (**7**). For the ruthenium cluster, the singlet state is found to be the ground state, with the first excited triplet state some 0.99 eV higher in energy. For the osmium analogue, the separation is even larger at 1.23 eV, consistent with the higher HOMO–LUMO separation in Figure 1. The difference between mononuclear and cluster systems is linked to the delocalization of the HOMO over ten metal atoms in the latter. Interelectron repulsion effects, which favor the high spin state, are therefore greatly reduced relative to mononuclear systems. In addition, the strongly covalent Ru–CO bonds will further reduce the interelectron repulsion within the metal d orbitals. The occupation of the excited triplet states will be negligible

even at ambient temperatures and cannot account for the reported Curie-type magnetic response of the osmium cluster. In light of these findings, we conclude that the temperature dependent responses of the lower nuclearity ruthenium clusters **11–14** and  $[\text{Os}_{10}(\mu_6\text{-C})(\text{CO})_{24}]^{2-}$  (**7**) must be due to some form of paramagnetic impurity in the samples, rather than indicating a transition towards metallic behavior as has been claimed previously. Consistent with this proposition, recent analyses by van Ruitenbeek and van Leeuwen of the size effect of the orbital magnetic susceptibility of small metallic systems has challenged the concept of a Curie-like domain with large clusters; instead, atomic-like properties are predicted to evolve gradually toward diamagnetic behavior close to the bulk Landau value.<sup>31</sup>

The EPR data from **2a** contradicts the magnetic susceptibility result; given that the latter is representative of the bulk sample, the temperature dependent Curie EPR signal for **2a** (and, by implication, that for **6d** and possibly for **9**) must be due to adventitious impurities. The lack of a temperature dependent EPR signal for **1a** is also strongly supportive of an adventitious source for the Curie signals in the isostructural **2a**, **6d**, and possibly **9**. Spin-orbit coupling has been suggested as the source of the paramagnetism leading to Curie signals;<sup>13(b)</sup> it is possible that large spin-orbit coupling for the third-row transition metal could lead to paramagnetism for moderate values of  $\Delta$ ,<sup>13(b)</sup> but this does not explain the existence of Curie signals for **2a** and **6d** but not for **1a**. It has been claimed that Curie signals are indicative of mesometallic character and are thus an indicator of approach to metallic behavior. If this is so, and osmium approaches metallic character at lower nuclearities than ruthenium, one would expect to see temperature-dependent Curie behavior at lower nuclearities for osmium than for ruthenium; magnetic susceptibilities are inconsistent with this. We conclude that the Curie signals are adventitious in origin.

The EPR spectra for **1a**, **2a**, and **6d** contain temperature-

independent signals, the first such reported for high-nuclearity carbonyl clusters. The LDF studies have shown that they cannot originate from metallic behavior, and the spin–spin relaxation rates are inconsistent with this possibility. Some other sources of the TIP response (solid-state packing, the unusual cation, and the presence of colloids, particles and oxides) have been eliminated from consideration by the EPR studies. The absence of a TIP EPR signal in previous work with osmium is suggestive of the TIP response arising from an impurity. The presence of the TIP EPR signal in frozen aliquots of centrifuged solutions of **1a** suggests soluble metal cluster carbonyl radical species as the likely source. It is perhaps significant that the osmium analogue **7** has been characterized in five oxidation states.<sup>33</sup> We are currently carrying out a detailed study of the electrochemistry of **1a** and its phosphine-substituted derivatives, together with UV-visible spectroelectrochemistry and EPR studies of the corresponding oxidized and reduced cluster complexes, to assess this possibility.<sup>34</sup>

**Acknowledgment.** We thank the Australian Research Council for support of this work, Johnson-Matthey for a loan of  $\text{RuCl}_3$ , Mr. D. Bogšányi and Dr. G. A. Heath for their assistance in obtaining the electronic spectra, Dr. R. J. Pace for access to the EPR spectrometer and ultracentrifuge, Ms. M. Karaman and Prof. R. M. Pashley for helpful discussions, and Ms. H. Thomas for assistance with the ultracentrifuge. M.P.C. held a UNE Postgraduate Research Scholarship, M.G.H. is an ARC Australian Research Fellow, and P.J.S. was the recipient of a Plant Science CRC Postgraduate Student Assistantship.

JA9602197

(33) Barley, M. H.; Drake, S. R.; Johnson, B. F. G.; Lewis, J. J. *Chem. Soc., Chem. Commun.* **1987**, 1657–59.

(34) Cifuentes, M. P.; Humphrey, M. G.; Heath, G. A., unpublished results.